

## Rheological properties of a vesicle suspension

M. Guedda,<sup>1,\*</sup> M. Benlahsen,<sup>2</sup> and C. Misbah<sup>3</sup>

<sup>1</sup>LAMFA, CNRS UMR 7352, Département de Mathématiques, Université de Picardie Jules Verne, Amiens F-80039, France

<sup>2</sup>LPMC, Département de Physique, Université de Picardie Jules Verne, Amiens F-80039, France

<sup>3</sup>Université de Grenoble/CNRS Laboratoire Interdisciplinaire de Physique (LIPhy), UMR 5588, Grenoble F-38041, France

(Received 7 July 2014; published 14 November 2014)

The rheological behavior of a dilute suspension of vesicles in linear shear flow at a finite concentration is analytically examined. In the quasispherical limit, two coupled nonlinear equations that describe the vesicle orientation in the flow and its shape evolution were derived [Phys. Rev. Lett. **96**, 028104 (2006)] and serve here as a starting point. Of special interest is to provide, for the first time, an exact analytical prediction of the time-dependent effective viscosity  $\eta_{\text{eff}}$  and normal stress differences  $N_1$  and  $N_2$ . Our results shed light on the effect of the viscosity ratio  $\lambda$  (defined as the inner over the outer fluid viscosities) as the main controlling parameter. It is shown that  $\eta_{\text{eff}}$ ,  $N_1$ , and  $N_2$  either tend to a steady state or describe a periodic time-dependent rheological response, previously reported numerically and experimentally. In particular, the shear viscosity minimum and the cusp singularities of  $\eta_{\text{eff}}$ ,  $N_1$ , and  $N_2$  at the tumbling threshold are brought to light. We also report on rheology properties for an arbitrary linear flow. We were able to obtain a constitutive law in a closed form relating the stress tensor to the strain rate tensor. It is found that the resulting constitutive law markedly contrasts with classical laws known for other complex fluids, such as emulsions, capsule suspensions, and dilute polymer solutions (Oldroyd B model). We highlight the main differences between our law and classical laws.

DOI: [10.1103/PhysRevE.90.052302](https://doi.org/10.1103/PhysRevE.90.052302)

PACS number(s): 83.50.Ha, 87.16.D–, 87.17.Jj

### I. INTRODUCTION

Vesicles (also known as fluid membranes) are closed membranes suspended in an aqueous medium and are similar, in some respects, to red blood cells (RBCs). They constitute an interesting viscoelastic model mimicking more complex entities. The dynamics of vesicles have been, and remain, a challenge for different disciplines ranging from biology to mathematics. The difficulty is due to the free-boundary character of the vesicles. The shape is not known *a priori* and is fixed or determined dynamically via a subtle interplay between the local flow and interfacial forces that gives rise to a large variety of shapes and dynamics, which have a strong impact on the suspension rheological behavior [1]. In the present paper we conduct a systematic study of a suspension of vesicles at a finite concentration as a function of the control parameter  $\lambda$  (the ratio between the viscosity of the encapsulated fluid over that of the suspending fluid), using analytical tools. In a general flow, the dynamics of vesicles seem to be a puzzle and the full equations of motion are intractable analytically and numerical treatments are inevitable. However, under certain asymptotic limits, the dynamics can be simplified.

Under a linear shear flow of the form  $\mathbf{u}_0 = (\dot{\gamma}y, 0, 0)$ , where  $\dot{\gamma}$  is the shear rate, vesicles (and RBCs) have been the subject of extensive theoretical, experimental, and numerical studies [2–24]. It is found that vesicles exhibit a variety of different regimes of motion depending on three control parameters: (i) the excess area  $\Delta = (A - 4\pi r_0^2)/r_0^2$ , (ii) the viscosity contrast  $\lambda = \eta_{\text{int}}/\eta_{\text{ext}}$ , and (iii) the bending number (or the dimensionless shear rate)  $C_\kappa = \eta_{\text{ext}}\dot{\gamma}r_0^3/\kappa$ , where  $A$  is the vesicle area,  $r_0 = [3V/(4\pi)]^{1/3}$ ,  $V$  is the volume of the vesicle,  $\eta_{\text{int}}$  and  $\eta_{\text{ext}}$  are the viscosities of the internal and

the external fluids, respectively, and  $\kappa$  is the bending rigidity modulus [25].

At low deformability (i.e.,  $C_\kappa$  is small), it is found that, in the shear plane, a quasispherical vesicle (i.e., its excess area  $\Delta$  is small) exhibits three major types of motions: (i) tank-treading (TT) mode, in which the vesicle deforms into a prolate ellipsoid inclined at a stationary angle  $\psi < \pi/4$  with the flow direction, while its membrane undergoes a tank-treading motion, (ii) tumbling (TB) mode, in which the membrane flips like a rigid body, and (iii) vacillating-breathing (VB) mode (sometimes called trembling or swinging), in which the main axis of the vesicle oscillates about the flow direction (the inclination angle  $\psi$  oscillates around 0 in the interval  $[-\pi/4, \pi/4]$ ), whereas its shape makes a breathing motion [13–15, 17, 20]. For small enough  $\lambda$ , vesicles exhibit the TT mode. Upon increasing the control parameter  $\lambda$ , the TT regime first becomes unstable in favor of the VB mode which loses in turn its stability in favor of the TB regime as  $\lambda$  increases. Furthermore, a remarkable property for a dilute suspension of vesicles was reported [15, 16, 20] (see also the recent papers by Veerapaneni *et al.* [23] and Thiébaud and Misbah [26]). From the numerical results the authors showed that the shear viscosity of a vesicle suspension first decreases, reaching a minimum, and suddenly increases with increasing  $\lambda$ . This minimum occurs at a critical value of  $\lambda$  corresponding to the transition between the TT and TB-VB regimes. In addition, it is found that the time-average of normal stress differences collapses in the TB and VB regime. This and some open questions formulated in Ref. [20] constituted the motivation for the present work.

Recently, we have shown in Ref. [27] that the original set of nonlinear differential equations can be analytically solved exactly in all the three regimes (TT, TB, and VB). Taking advantage of this solution, we show here that all rheological properties (steady and time-dependent) can be expressed exactly analytically. Note that until now, analytical expressions were only known in the TT regime [13]. Our study

\*guedda@u-picardie.fr

will provide a clear picture of all the reported numerical results about rheology. Another important aspect reported here is the derivation of a constitutive law in a closed form relating the stress tensor to the strain rate tensor. It will be recognized that the present law differs from those known for emulsion or polymer solutions (Oldroyd B model). The main difference is attributed to local membrane incompressibility.

The paper is structured as follows: Section II deals with a brief description of the small-deformation theory [13], followed by a short presentation of the expression of the exact analytical solutions, which was the subject of our previous paper [27]. Section III presents the results for rheology of a dilute vesicle suspension. In Sec. IV, we report on rheology properties for an arbitrary linear flow and, in Sec. V, we compare them with emulsions, capsule suspensions and dilute polymer solutions. Finally, Secs. VI and VII contain the summary of the main results and conclusion and perspectives, respectively.

## II. DYNAMICS UNDER SHEAR FLOW

Before starting the discussion of rheology, some preliminaries about the considered context are necessary. To analytically analyze TT, TB, and VB regimes a nearly spherical vesicle shape is considered [13]. At small deformation it is found that the vesicle deformation is described by the radial position  $r$  of the vesicle interface which can be presented as ( $r_0 = 1$ )

$$\begin{aligned} r &= 1 + F_{2-2}\mathcal{Y}_2^{-2} + F_{20}\mathcal{Y}_2^0 + F_{22}\mathcal{Y}_2^2, \\ r &= 1 + \mathcal{R}[\cos(2\psi) + i \sin(2\psi)]\mathcal{Y}_2^{-2} + F_{20}\mathcal{Y}_2^0 \\ &\quad + \mathcal{R}[\cos(2\psi) - i \sin(2\psi)]\mathcal{Y}_2^2, \end{aligned} \quad (1)$$

where  $\mathcal{Y}_2^m, m = -2, 0, 2$ , are the usual spherical harmonics of order two,  $\psi$  coincides with the orientation angle of the vesicle in  $x$ - $y$  plane, and  $\mathcal{R}$  and  $F_{20}$  are the (real) amplitudes of deformation of the vesicles. The quantity  $F_{2-2}\mathcal{Y}_2^{-2} + F_{20}\mathcal{Y}_2^0 + F_{22}\mathcal{Y}_2^2$ , which is assumed to be small, is the deviation of the vesicle shape from a sphere of equivalent volume. In Ref. [13], it is found that  $\psi$  and  $\mathcal{R}$  satisfy

$$\begin{aligned} \frac{d\mathcal{R}}{dt} &= h \left[ 1 - 4 \frac{\mathcal{R}^2}{\Delta} \right] \sin(2\psi) \\ \frac{d\psi}{dt} &= -\frac{1}{2} + \frac{h}{2\mathcal{R}} \cos(2\psi), \end{aligned} \quad (2)$$

where  $h = 60\sqrt{2\pi/15}/(32 + 23\lambda)$ . The above system constitutes the basic equations in the small-deformation theory. One key challenge is the highly nonlinear character of system Eq. (2). This is traced back to the constraint of local-area incompressibility. Note that system (2) is free of  $\kappa$  or, more precisely, free of  $C_\kappa$ .

$F_{20}$  is connected to  $\mathcal{R}$  via the area conservation constraint [13]

$$\Delta = 4\mathcal{R}^2 + 2F_{20}^2, \quad (3)$$

which reflects the fact that the deformation amplitudes must comply with the available excess area. If there is no deformation along the vorticity direction (i.e.,  $F_{20} = 0$ ) we have  $\mathcal{R} = \sqrt{\Delta}/2$  (fixed vesicle shape). In this case the orientation angle satisfies the Keller–Skalak (KS) phenomenological model (the

Jeffery equation)

$$\frac{d\psi}{dt} = -\frac{1}{2} + \frac{h}{\sqrt{\Delta}} \cos(2\psi), \quad (4)$$

which describes the dynamics of TT and TB motions with fixed shape [2]. The TT motion is predicted when  $\lambda$  is less than a critical value  $\lambda_c$  (see below), and the TB motion occurs when  $\lambda > \lambda_c$ .

To put our present study in the context of earlier works, we give a brief description of recent and known results concerning system (2). In Ref. [13] the author showed that the critical viscosity ratio which separates the TT and TB regimes is given by

$$\lambda_c = -32/23 + (120/23)\sqrt{2\pi/15\Delta}. \quad (5)$$

More precisely, for  $\lambda < \lambda_c$ , or  $h > \sqrt{\Delta}/2 \equiv h_c$ , system (2) has the equilibrium points

$$\mathcal{R}_0 = \frac{\sqrt{\Delta}}{2}, \quad \psi_0 = \pm \frac{1}{2} \cos^{-1} \left( \frac{\sqrt{\Delta}}{2h} \right). \quad (6)$$

The “+” fixed point is stable and the “−” fixed point is unstable.

For  $h < h_c$ , there is no fixed-orientation solution. Instead, an unsteady tumbling motion is found. It is shown that the TB mode takes place and coexists with the VB mode [14,15,17,18,20,23].

Besides the numerical investigations, a complete set of exact closed solutions for the vesicle orientation and its shape evolution were recently presented by Guedda *et al.* [27] using elementary methods. For later purposes we need to recall some of the aspects. The essential idea is to introduce new independent variables which transform the original system into a system which is easier to solve. The authors noted that system (2) can be simply rewritten as

$$\begin{aligned} \frac{d\xi}{dt} &= \zeta \left( 1 - \frac{4h}{\Delta} \xi \right) \\ \frac{d\zeta}{dt} &= h - \xi - \frac{4h}{\Delta} \zeta^2, \end{aligned} \quad (7)$$

in new independent variables  $\xi = \mathcal{R} \cos(2\psi)$  and  $\zeta = \mathcal{R} \sin(2\psi)$ . The shape deformation and the inclination angle are given by  $\mathcal{R}^2 = \xi^2 + \zeta^2$  and  $\psi = \frac{1}{2} \arctan(\zeta/\xi)$ . It is found for  $h > h_c$  that

$$\begin{aligned} \zeta(t) &= \frac{\Delta\omega}{4h} \frac{e^{\omega t} - C_1 e^{-\omega t}}{C_2 + e^{\omega t} + C_1 e^{-\omega t}}, \\ \xi(t) &= \frac{\Delta}{4h} + \frac{\omega^2 \Delta}{4h} \frac{C_2}{C_2 + e^{\omega t} + C_1 e^{-\omega t}}, \end{aligned} \quad (8)$$

whereas for  $h < h_c$ ,

$$\begin{aligned} \zeta(t) &= \frac{\Delta\omega}{4h} \frac{\cos(\omega t + C_3)}{C_4 + \sin(\omega t + C_3)}, \\ \xi(t) &= \frac{\Delta}{4h} \frac{\Gamma + \sin(\omega t + C_3)}{C_4 + \sin(\omega t + C_3)}, \\ \Gamma &= \frac{4h^2}{\Delta} C_4, \end{aligned} \quad (9)$$

where  $\omega = |1 - \frac{4h^2}{\Delta}|^{1/2}$  and  $C_j, j = 1, 2, 3, 4$ , are constants depending on the initial conditions.

For  $h > h_c$  (TT regime), the inclination angle  $\psi$  follows from Eq. (8) as

$$\psi(t) = \frac{\pi}{4} - \frac{1}{2} \arctan\left(\frac{4h^2 C_2 + \Delta[e^{\omega t} + C_1 e^{-\omega t}]}{\omega \Delta[e^{\omega t} - C_1 e^{-\omega t}]}\right). \quad (10)$$

From Eq. (8) we may deduce that  $\zeta$  and  $\xi$  tend to

$$\xi_\infty = \frac{\Delta}{4h}, \quad \zeta_\infty = +\frac{\Delta}{4h} \sqrt{\frac{4h^2}{\Delta} - 1}, \quad (11)$$

respectively, as  $t$  tends to infinity, and then (as is known)  $\mathcal{R}$  goes to  $\sqrt{\Delta}/2$  and  $\psi$  approaches the limit value

$$\psi_\infty = \frac{\pi}{4} - \frac{1}{2} \arctan(\omega^{-1}) = +\frac{1}{2} \cos^{-1}\left(\frac{\sqrt{\Delta}}{2h}\right), \quad (12)$$

as  $t$  tends to infinity. The asymptotic solution corresponds to a pure TT solution.

For  $h < h_c$  (during TB and VB regimes) it is found that the inclination angle satisfies

$$\psi(t) = \frac{\pi}{4} \frac{\Gamma}{|\Gamma|} \frac{\cos(\omega t + C_3)}{|\cos(\omega t + C_3)|} \left[ 1 - \frac{\Gamma}{|\Gamma|} \frac{\Gamma + \sin(\omega t + C_3)}{|\Gamma + \sin(\omega t + C_3)|} \right] + \frac{1}{2} \arctan\left(\omega \frac{\cos(\omega t + C_3)}{\Gamma + \sin(\omega t + C_3)}\right). \quad (13)$$

The above expression is an extension of the KS solutions which was obtained under the shape-preserving assumption. Our solution accounts not only for the inclination angle but also for shape evolution [27]. Note that the shape deformation  $\mathcal{R}$  can be written as (during oscillating regimes)

$$\mathcal{R}^2(t) = \frac{\Delta}{4} + \frac{\omega^2 \Delta^3}{64h^4} \left[ \frac{4h^2}{\Delta} - \Gamma^2 \right] \frac{1}{[C_4 + \sin(\omega t + C_3)]^2}. \quad (14)$$

The above equation implies that  $|\Gamma| \geq \frac{2h}{\sqrt{\Delta}} \equiv \Gamma_c$  by using constraint (3) and shows, in particular, the role of  $\Gamma$  in causing departure from the KS model and that  $\mathcal{R} = \frac{\sqrt{\Delta}}{2}$  (shape-preserving regime) only for  $\Gamma = \pm \Gamma_c$ . From Eq. (13) two qualitatively different solutions are obtained by varying  $\Gamma$ .  $\Gamma_c \leq |\Gamma| < 1\psi$  describes a TB regime, while a VB regime is obtained if  $|\Gamma| > 1$ . The border, or the TB to VB transition, separating VB and TB regimes is obtained if  $\Gamma = \pm 1$ . We suppose here that  $\Gamma > 0$ .

### III. RHEOLOGY OF VESICLE SUSPENSION

Once the exact expressions of solutions of each regime are obtained, the rheology of a dilute suspension will be easily analyzed. Of particular interest are the steady and the time-dependent effective viscosity (which is given by the shear stress divided by strain rate), and the first normal stress difference  $N_1 = \sigma_{11} - \sigma_{22}$  and the second normal stress difference  $N_2 = \sigma_{22} - \sigma_{33}$ , where “1, 2, 3” designate the flow, the shear gradient, and the vorticity direction, respectively. In fact, the basic question that underlines this section is how do the effective viscosity and normal stress differences for a dilute suspension behave at any time in the three primary regimes (TT, TB, and VB)?

#### A. Reduced effective viscosity

In Ref. [19], Vitkova *et al.* reported on experimental observations of the reduced effective viscosity, or the normalized viscosity,

$$[\eta] = \frac{\eta_{\text{eff}} - \eta_{\text{ext}}}{\eta_{\text{ext}} \varphi}, \quad (15)$$

for vesicles and RBCs. In Eq. (15),  $\eta_{\text{eff}}$  is the time-dependent effective viscosity and  $\varphi$  is the volume fraction of the suspension (the volume occupied by the vesicles over the total volume). Vitkova *et al.* observed that the reduced effective viscosity of a vesicle suspension follows the general trend of a RBC suspension with a slow decrease in the TT regime and a rapid increase after the transition to TB. For quasispherical vesicles, Danker and Misbah [15] and Danker *et al.* [20] derived the formal expression of the time-dependent effective viscosity

$$\eta_{\text{eff}}(t) = \eta_{\text{ext}} \left[ 1 + \frac{5}{2} \varphi \left( 1 - \frac{4}{5} \sqrt{\frac{15}{2\pi}} h \right) + \frac{\varphi}{\Delta} h \sqrt{\frac{480}{\pi}} \mathcal{R}^2(t) \sin^2(2\psi) \right], \quad (16)$$

or, equivalently,

$$\eta_{\text{eff}}(t) = \eta_{\text{ext}} \left[ 1 + \frac{5}{2} \varphi \left( 1 - \frac{4}{5} \sqrt{\frac{15}{2\pi}} h \right) + \frac{\varphi}{\Delta} h \sqrt{\frac{480}{\pi}} \zeta^2(t) \right]. \quad (17)$$

The reduced effective viscosity reads

$$[\eta] = \frac{5}{2} \left( 1 - \frac{4}{5} \sqrt{\frac{15}{2\pi}} h \right) + \frac{h}{\Delta} \sqrt{\frac{480}{\pi}} \zeta^2(t). \quad (18)$$

The last term of Eq. (18), which is nonlinear, represents the contributions of the vesicle deformation and orientation. The time-dependent effective viscosity and the reduced effective viscosity are evaluated here by using the exact expression of  $\zeta$ . As the explicit solutions were not known before the authors of Refs. [15,20] presented the reduced effective viscosity for the steady TT regime:

$$[\eta] = \frac{5}{2} - \Delta \frac{23\lambda + 32}{16\pi}. \quad (19)$$

For the unsteady regimes, system (2) has been solved numerically and the time-average of  $[\eta]$  over one period has been determined. This quantity is a function of  $\lambda$  and  $\Delta$ , for the three regimes, and is denoted  $\langle [\eta] \rangle$ . It is found that  $\langle [\eta] \rangle$  decreases with increasing  $\lambda$  and attains a minimum at  $\lambda_c$ . For  $\lambda > \lambda_c$ ,  $\langle [\eta] \rangle$  exhibits a sudden increase, in agreement with experiments [19]. In addition, it is found that the TB regime possesses a higher viscosity than the TT regime at the same distance from the bifurcation point (see Fig. 2 of Ref. [15] and Fig. 6 of Ref. [23]).

Here, as mentioned above, we use the exact explicit solutions (for the three regimes) in the calculation of  $[\eta]$ , focusing on the dependence on viscosity parameter  $h$  or viscosity ratio  $\lambda$ . We shall see briefly, as is known, that the behaviors of the reduced viscosity as a function of  $\lambda$

for a suspension of vesicles and for an emulsion are quite different. A general comparison with some complex fluids can be found in Secs. IV and V. Actually, since the “+” steady TT motion (11) is stable, one sees that  $\eta_{\text{eff}}(t)$  goes to

$$\eta_{\text{eff}}(\infty) = \eta_{\text{ext}} \left[ 1 + \frac{5}{2} \varphi \left( 1 - \frac{4}{5} \sqrt{\frac{15}{2\pi}} h \right) + \varphi \sqrt{\frac{15}{8\pi}} \frac{4h^2 - \Delta}{h} \right], \quad (20)$$

as  $t$  tends to infinity. Thereafter, reduced effective  $[\eta]$  approaches Eq. (19) for  $t$  large enough.

Let us now evaluate the time-dependent effective viscosity. Making use of Eq. (18), one sees from Eqs. (8) and (9) that

$$[\eta] = \frac{5}{2} \left( 1 - \frac{4}{5} \sqrt{\frac{15}{2\pi}} h \right) + |4h^2 - \Delta| \sqrt{\frac{480}{\pi}} \frac{1}{16h} \mathcal{G}(\omega t), \quad (21)$$

where the function  $\mathcal{G}$  is given by

$$\mathcal{G}(t) = \frac{(e^t - C_1 e^{-t})^2}{(C_2 + e^t + C_1 e^{-t})^2} \quad (22)$$

for  $\lambda < \lambda_c$  and, for  $\lambda > \lambda_c$ ,

$$\mathcal{G}(t) = \frac{\cos^2(t + C_3)}{[C_4 + \sin(t + C_3)]^2}. \quad (23)$$

Expression (21) displays several interesting properties. As a function of  $t$ , the reduced effective viscosity for a TB or VB regime exhibits a minimum over one period [15,28]. This minimum, which is given by

$$[\eta]_{\text{min}} = \frac{5}{2} \left( 1 - \frac{4}{5} \sqrt{\frac{15}{2\pi}} h \right), \quad (24)$$

irrespective of  $\Gamma$ , occurs at  $\psi = 0, \pm \pi/2$  during the TB regime, while during the VB regime the minimum occurs at  $\psi = 0$ . On the other hand, by using Eq. (21), one sees that the maximum value over one period of the reduced effective viscosity is given by

$$[\eta]_{\text{max}} = \frac{5}{2} \left( 1 - \frac{4}{5} \sqrt{\frac{15}{2\pi}} h \right) + \frac{|4h^2 - \Delta|}{\Gamma^2 \Delta^2 - 16h^4} h^3 \sqrt{\frac{480}{\pi}}, \quad (25)$$

which decays monotonically as  $\Gamma$  increases and tends to Eq. (24) as  $\Gamma$  tends to infinity. We plotted in Fig. 1 the time evolution of the reduced effective viscosity (during periodic regimes) for different values of the parameter  $\Gamma$  ( $\Gamma = \frac{4h^2}{\Delta} C_4$ ). Equation (25) indicates that the maximum possible of the instantaneous reduced effective viscosity is attained if  $\Gamma = \Gamma_c$ , corresponding to the shape-preserving regime, and this maximum value is  $5/2$ .

Next, as in Ref. [20], we are also interested in the time average over one period. From Eq. (22) we get

$$\langle [\eta] \rangle = \frac{5}{2} \left( 1 - \frac{4}{5} \sqrt{\frac{15}{2\pi}} h \right) + |4h^2 - \Delta| \sqrt{\frac{480}{\pi}} \frac{1}{16h} M(\mathcal{G}), \quad (26)$$

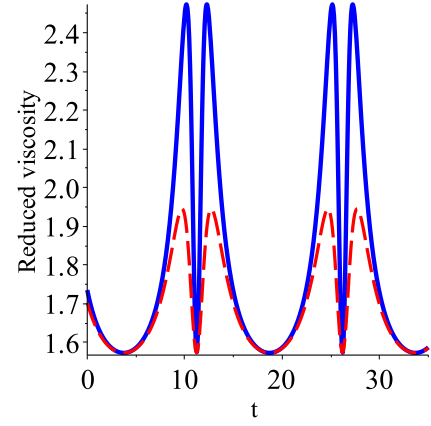


FIG. 1. (Color online) Time-dependent reduced viscosity  $[\eta]$  during TB and VB regimes for different values of  $\Gamma$ . Parameters are  $\Delta = 0.437$ ,  $h = 0.3$ ,  $\Gamma = 0.91$  (solid blue line), and  $\Gamma = 1.02$  (dashed red line).

where ( $C_4 > 1$ )

$$M(\mathcal{G}) = \frac{C_4 - \sqrt{C_4^2 - 1}}{\sqrt{C_4^2 - 1}}, \quad (27)$$

for  $h < h_c$  (during TB and VB regimes), and for  $h > h_c$  (at steady state)

$$\langle [\eta] \rangle = \frac{5}{2} - \frac{\Delta}{4h} \sqrt{\frac{30}{\pi}}. \quad (28)$$

The above expression, which extends the famous Einstein result [29] for particle suspensions to the case of vesicles, was originally derived in Ref. [13]. Note that this expression remains valid in the limit of the spherical case  $\Delta = 0$ , irrespective of the value of  $\lambda$ , since a sphere with fixed area and volume in shear flow only undergoes a rigid body rotation. This is a peculiar property of the presence of a membrane.

If  $\Gamma = \Gamma_c$  (shape-preserving solution) we have

$$\langle [\eta] \rangle = \frac{5}{2} \left( 1 - \frac{4}{5} \sqrt{\frac{15}{2\pi}} h \right) + h \frac{\sqrt{\Delta - 4h^2}}{\sqrt{\Delta} + \sqrt{\Delta - 4h^2}} \sqrt{\frac{30}{\pi}}. \quad (29)$$

A similar expression has been derived in Ref. [19] in the small-capillary-number (see below) limit where a direct transition from TT to TB occurs.

As is readily apparent from Eq. (26) the reduced effective viscosity first decreases, reaching the minimum

$$\langle [\eta] \rangle_{\text{min}} = \frac{5}{2} - \sqrt{\frac{15\Delta}{2\pi}} \quad (30)$$

at the critical value  $\lambda = \lambda_c$ , and then increases with increasing  $\lambda$ , with a cusp singularity at  $\lambda = \lambda_c$ . The reduced average effective viscosity, as a function of  $h$ , is plotted in Fig. 2.

Next, we consider the two limiting cases  $\lambda \rightarrow \infty$  (high internal rigidity) and  $\lambda \rightarrow 0$  (small internal rigidity). For large

enough  $\lambda$ , we first note that

$$\frac{5}{2} \left( 1 - \frac{4}{5} \sqrt{\frac{15}{2\pi}} h \right) \leq [\eta] \leq \frac{5}{2} \quad (31)$$

for the three regimes. Estimate (31) says that the vesicle suspension cannot exceed the Einstein viscosity (at leading order). Using Eq. (31) one may see that  $[\eta]$  tends to  $5/2$  as  $h$  approaches 0 or  $\lambda \rightarrow \infty$ . In the opposite limit,  $\lambda \rightarrow 0$ , since the vesicle performs the TT regime we deduce from Eq. (19) that  $[\eta]$  tends to  $5/2 - 2\Delta/\pi$  (see also the numerical simulations of Ref. [16]). Note that this limiting value decreases upon increasing  $\Delta$  and approaches  $5/2$  as  $\Delta$  tends to 0 (rigid body rotation). The same conclusion was reached numerically for a dilute suspension in two dimensions [28]. It is found that the reduced suspension viscosity of quasicircular vesicle approaches 2 (which is the Einstein result in two dimensions) for large enough  $\lambda$ , and for  $\lambda \rightarrow 0$  it approaches a limiting value that decreases upon decreasing the reduced area  $\nu$ , defined as  $\nu = A/(\pi[p/2\pi]^2)$ , where  $A$  is the vesicle area and  $p$  is the vesicle perimeter. Moreover, it is observed that this limiting value (at  $\lambda = 0$ ) tends to 2 as  $\nu \rightarrow 1$  (corresponding to a circle). This limiting value is the effective viscosity of a dilute suspension of rigid circle (for the  $d$ -dimensional spherical particles, Brady [30] showed that the Einstein coefficient is equal to  $1 + d/2$ ). An extensive physical comparison between emulsion and vesicle suspension in two dimensions can be found in Ref. [28].

### B. Comparison with initially spherical capsules with a red-blood-cell-type membrane

In the spirit of Ref. [20], we would like to compare the reduced effective viscosity of vesicles at leading order to that of an initially spherical capsule, in order to tentatively analyze the similarity and/or the dissimilarity between the excess area for vesicles and the elastic capillary number for capsules  $Ca = \eta_{\text{ext}} \dot{\gamma} r_0 / \mu$ , where  $\mu$  is the shear elastic modulus. We recall, as mentioned in Ref. [14], that in the small-deformation approach for initially spherical capsules, the capillary number or the inverse viscosity ratio are used as the small parameters of the expansion, while for vesicles the small parameter is  $\sqrt{\Delta}$ .

Recently, numerical studies on the rheology of a dilute suspension of initially spherical capsules with both Skalak (SK) and neo-Hookean (NH) laws have been presented by Bagchi and Kalluri [31]. The authors considered a physical situation for which only the steady TT motion is observed and analyzed the behavior of the reduced effective viscosity as a function of the viscosity ratio and the elastic capillary number. For example, for the SK model, the authors concluded that for  $Ca \leq 0.1$  the reduced effective viscosity decreases uniformly with increasing  $\lambda$ , while for  $Ca > 0.1$  the reduced effective viscosity first decreases reaching a (smooth) minimum, and then increases with increasing  $\lambda$ . This indicates, in particular, that a capsule suspension may exhibit a shear viscosity minimum, even when the capsule is in TT regime, unlike a vesicle suspension at leading order [15].

For the present comparison, we focus on an initially spherical capsule with a RBC-type membrane, since an analytical expression of the reduced effective viscosity is obtained. Based

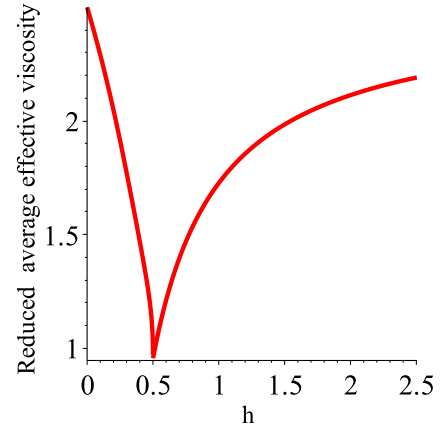


FIG. 2. (Color online) Reduced average effective viscosity  $\langle [\eta] \rangle$  as a function of  $h$  for  $\Delta = 1$ . The cusp singularity is due to the transition from TB or VB to TT.

on the work of Barthes-Biesel and Rallison [32], Drochon [32] derived the following analytical expression for the reduced effective viscosity  $[\eta^c]$  for an initially spherical capsule with a RBC-type membrane:

$$[\eta^c] = \frac{5}{2} \frac{23\lambda - 16}{23\lambda + 32} + \frac{7680}{(23\lambda + 32)[64 + (23\lambda + 32)^2 Ca^2]}, \quad (32)$$

for small  $Ca$ . Moreover, Drochon proposed to use Eq. (32) as a phenomenological equation to predict rheological properties of RBCs even if elastic capillary number  $Ca$  is not small. Behaviors of  $[\eta^c]$  as a function of  $Ca$  are plotted for  $\lambda = 0.2$  and  $\lambda = 1$  (see Fig. 4 of Ref. [32] of Drochon). The high-shear limit ( $Ca \rightarrow \infty$ ) of  $[\eta^c]$  is also obtained from Eq. (32). It must be noted that Eq. (32) has already been found by Barthes-Biesel in Ref. [33].

As in Ref. [31], we analyze the qualitative behavior of  $[\eta^c]$ , as a function of  $\lambda$ , a property that is not presented in Refs. [32] and [33]. From Eq. (32) we find that

$$\frac{\partial}{\partial \lambda} [\eta^c] = 2760 \frac{(23\lambda + 32)^2 Ca^2 - 64}{[(23\lambda + 32)^2 Ca^2 + 64]^2} Ca^2, \quad (33)$$

showing that, at finite  $Ca > 0$ ,  $[\eta^c]$  exhibits a smooth minimum (see Fig. 3)

$$[\eta^c]_{\min} = \frac{5}{2}(1 - 3Ca), \quad (34)$$

and, at the critical value,

$$\lambda_c^* = \frac{8}{23}(Ca^{-1} - 4). \quad (35)$$

As a result, we can distinguish two different trends depending on the value of  $Ca$ . For values of  $Ca$  in the range  $Ca \geq 0.25$ , the critical value  $\lambda_c^*$  is negative. This means that  $[\eta^c]$  increases uniformly with increasing  $\lambda$ . In the range  $Ca < 0.25$ ,  $[\eta^c]$  presents some similarities with the predictions of Danker and Misbah [15], Danker *et al.* [20], and Bagchi and Kalluri [31];  $[\eta^c]$  first decreases reaching the minimum (34), and then increases with  $\lambda$ . Figure 3 shows the effect of  $\lambda$  for various  $Ca$ . Note that, as in Ref. [31], the minimum of  $[\eta^c]$  decreases as  $Ca$  increases, and that for small enough  $Ca$  there is a long interval where  $[\eta^c]$  decreases before reaching the minimum (34).

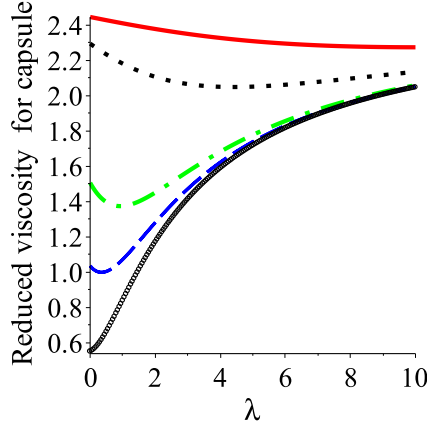


FIG. 3. (Color online) Reduced viscosity for capsules with a RBC-type membrane as a function of the viscosity ratio for different values of  $Ca$ :  $Ca = 0.06$  (solid red line),  $0.1$  (dotted black line),  $0.15$  (dotted-dashed green line),  $0.2$  (dashed blue line), and  $0.26$  (circle black line).

Notice again that  $[\eta^c]$  is negative for small enough  $\lambda$  for  $Ca > \sqrt{2}/4 \approx 0.3535$  [see Eq. (37) below]. However, as for vesicles with moderate reduced volume [34], the behavior of Eq. (32) agrees at least qualitatively with the results for capsules reported by Bagchi and Kalluri [31].

As for vesicles, the reduced effective viscosity  $[\eta^c]$  satisfies Eq. (31), i.e.,

$$\frac{5}{2} \left( 1 - \frac{4}{5} \sqrt{\frac{15}{2\pi}} h \right) \leq [\eta^c] \leq \frac{5}{2}, \quad (36)$$

and then approaches  $5/2$  as  $h$  tends to 0, or  $\lambda \rightarrow \infty$ . For  $\lambda \rightarrow 0$  we have

$$[\eta^c] = \frac{5}{2} \left( 1 - \frac{24Ca^2}{1 + 16Ca^2} \right). \quad (37)$$

The above limiting behavior, which is below the Einstein value, increases upon decreasing  $Ca$ , and approaches the Einstein value for small enough  $Ca$ . A similar behavior is predicted in the small-deformation theory of spherical microcapsule suspensions [35]. In fact, as in Ref. [35] and as pointed out in Ref. [32], we can see from Eq. (32) that, in the low-shear limit,  $[\eta^c] = 5/2$  in all cases.

Analogous to Ref. (35), the critical value  $\lambda_c$  for vesicle [Eq. (5)] can be written as

$$\lambda_c = \frac{8}{23}(\delta^{-1} - 4), \quad (38)$$

where

$$\delta = \sqrt{\frac{\Delta}{30\pi}}. \quad (39)$$

Hence, for  $\delta > 1/4$  the reduced effective viscosity  $[\eta]$  for vesicles increases uniformly with increasing  $\lambda$ , and if  $\delta < 1/4$ ,  $[\eta]$  first decreases reaching the minimum (34), and then increases with  $\lambda$  in the VB and TB regimes. Therefore, we may deduce, at first sight, that  $Ca$  and  $\delta$  play a similar role.

In this respect, there is some qualitative similarity between vesicles (at leading order) and initially spherical capsules with a RBC-type membrane. However, their physical mechanisms

are different. The reduced viscosity for vesicles reaches the minimum at the TT-to-TB transition, which is associated with the onset of the VB mode [15,16], while for initially spherical capsules with a RBC-type membrane the minimum may occur even if the capsules are in a steady tank-treading regime. A similar trend was reported in numerical studies for vesicles in Ref. [16]. In that paper the authors discussed the implication of the higher-order theory on the rheology of vesicles as a function of  $\lambda$ . It is predicted that, at small bending number  $C_\kappa$ , the cusp singularity persists as in the leading order, while at larger  $C_\kappa$ , the cusp is smeared out and, in addition, the minimum is located in the TT mode.

Let us continue our comparison. It is worth noting here that the critical value for capsule  $\lambda_c^*$  (35) coincides with  $\lambda_c$  for vesicles (38) if  $Ca$  is proportional to  $\sqrt{\Delta}$ , i.e.,

$$Ca = \sqrt{\frac{\Delta}{30\pi}} = Ca^*. \quad (40)$$

In this case minimum (34) reads

$$[\eta^c]_{\min} = \frac{5}{2} \left( 1 - 3\sqrt{\frac{\Delta}{30\pi}} \right), \quad (41)$$

which is larger than quantity  $([\eta])_{\min}$  given in Eq. (30) except if  $\Delta = 0$ . We note that

$$\lambda_c^* \sim \frac{8}{23} Ca^{-1} \quad (42)$$

as  $Ca$  goes to 0 and

$$\lambda_c \sim \frac{8}{23} \sqrt{\frac{30\pi}{\Delta}} = \frac{8}{23} (Ca^*)^{-1} \quad (43)$$

as  $\Delta$  goes to 0.

We note again that the minimum (34) for capsules coincides with that for vesicles [Eq. (30)] if

$$Ca = 2\sqrt{\frac{\Delta}{30\pi}}, \quad (44)$$

which is nearly the critical elastic capillary number, derived in Ref. [24], for the transition from swinging to TB for a nonspherical microcapsule at small enough  $\Delta$  [see Eq. (4.12) of Ref. [24]].

For the sake of completeness, we note a formal analogy between the vesicle and capsule problems. The reduced effective viscosities can be written as (after using the definition of  $h$ )

$$[\eta^c] = \frac{5}{2} \frac{23\lambda - 16}{23\lambda + 32} + \frac{120}{23\lambda + 32} \frac{1}{1 + (23\lambda + 32)^2 (Ca/8)^2} \quad (45)$$

for capsules with a RBC-type membrane and, for vesicles, as

$$\langle [\eta] \rangle = \frac{5}{2} \frac{23\lambda - 16}{23\lambda + 32} + \frac{120}{23\lambda + 32} \frac{4}{\Delta} \langle \zeta^2 \rangle. \quad (46)$$

For the shape-preserving solution the above expression reads

$$\langle [\eta] \rangle = \frac{5}{2} \frac{23\lambda - 16}{23\lambda + 32} + \frac{120}{23\lambda + 32} \frac{1}{1 + \frac{\sqrt{\Delta}}{\sqrt{\Delta - 4h^2}}}. \quad (47)$$

During the VB to TB transition ( $\Gamma = 1$ ) the maximum value (over one period) of the instantaneous reduced effective viscosity can also be written as

$$[\eta]_{\max} = \frac{5}{2} \frac{23\lambda - 16}{23\lambda + 32} + \frac{120}{23\lambda + 32} \frac{1}{1 + \frac{\Delta}{4h^2}}. \quad (48)$$

As in Eqs. (47) and (48), the terms proportional to  $\frac{120}{23\lambda + 32}$  in both equations (45) and (46) take values in the interval (0, 1). This may suggest that Eqs. (45) and (46) are similar. In fact, Eq. (45) is equal to Eq. (46) if

$$\frac{1}{1 + (23\lambda + 32)^2 (Ca/8)^2} = \frac{4}{\Delta} \langle \zeta^2 \rangle. \quad (49)$$

In the stationary state (6), relation (49) holds for

$$Ca^{-1} = \frac{1}{h} \sqrt{\frac{15\pi}{2}} \sqrt{\frac{4h^2}{\Delta} - 1} \quad (50)$$

or, equivalently,

$$Ca^{-1} = 2\sqrt{\frac{15\pi}{2\Delta}} \sqrt{1 - \Delta \left( \frac{23\lambda + 32}{8\sqrt{30\pi}} \right)^2}. \quad (51)$$

At small enough  $\Delta$  we have  $Ca \sim Ca^*$  [see Eq. (40)]. The same estimate holds at the bifurcation from VB to TB. More precisely, Eq. (45) coincides with Eq. (48) [the maximum value (over one period) of the instantaneous reduced effective viscosity] if  $Ca = Ca^*$ . This result indicates, in particular, that if  $Ca < Ca^*$  we have  $[\eta] < [\eta^c]$  during VB regimes.

Finally, In the limit  $Ca \rightarrow 0$  (for fixed  $\Delta$ ), since very small  $Ca$  corresponds to quasirigid particles, we use Eq. (47) to deduce that the behaviors of the reduced viscosity for a suspension of vesicles and for a suspension of initially spherical capsules with a RBC-type membrane are closely similar for large  $\lambda$  or small  $h$  if

$$Ca^{-2} = \frac{15\pi}{2h^2} \sqrt{1 - \frac{4h^2}{\Delta}}. \quad (52)$$

Not surprisingly, we get from Eq. (52) that  $Ca$  goes to zero with  $h$  or, equivalently, as  $\lambda \rightarrow \infty$ , and then

$$Ca \sim \frac{8}{23} \lambda^{-1}, \quad (53)$$

as  $\lambda \rightarrow \infty$ . Relation (53), which is similar to Eq. (42), was used in Ref. [32] in the case of highly viscous capsules. In that case both  $[\eta^c]$  and  $[\eta]$  have the same limiting value  $5/2$  as  $\lambda \rightarrow \infty$ .

### C. Normal stress differences

As an interesting supplemental physical investigation and another consequence of the exact explicit solutions is to compute the first normal stress difference  $N_1 = \sigma_{11} - \sigma_{22}$  and the second normal stress difference  $N_2 = \sigma_{22} - \sigma_{33}$ . According to Ref. [15],  $N_1$  and  $N_2$  are given by

$$N_1 = -2N_2 = \frac{16\varphi\dot{\gamma}\eta_{\text{ext}}}{\Delta} \sqrt{\frac{15}{32\pi}} \mathcal{R}^2 \sin(4\psi). \quad (54)$$

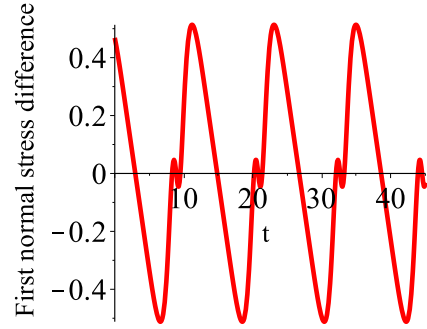


FIG. 4. (Color online) Time evolution of the first normal stress difference for  $\Delta = 0.5$ ,  $h = 0.3$ , and  $\Gamma = 0.95$  (tumbling regime). Parameters  $\varphi$ ,  $\eta_{\text{ext}}$ , and  $\dot{\gamma}$  are such that  $\varphi\eta_{\text{ext}}\dot{\gamma} = 0.2$ .

By using the identity  $\sin(2x) = 2 \sin x \cos x$ , Eq. (54) can be written simply as

$$N_1 = -2N_2 = \frac{32\varphi\dot{\gamma}\eta_{\text{ext}}}{\Delta} \sqrt{\frac{15}{32\pi}} \xi \zeta. \quad (55)$$

Therefore, in the TT regime,  $N_1$  approaches

$$N_1(\infty) = \varphi\dot{\gamma}\eta_{\text{ext}} \sqrt{\frac{15\Delta}{2\pi}} \frac{1}{h^2} \sqrt{h^2 - h_c^2} \quad (56)$$

as  $t$  tends to infinity. In the TB and VB regimes the exact solution (9) yields

$$N_1 = -2N_2 = \frac{\varphi\dot{\gamma}\eta_{\text{ext}}}{2} \sqrt{\frac{15}{2\pi}} \frac{\Delta}{h^2} \times \frac{\cos(\omega t + C_3)[\Gamma + \sin(\omega t + C_3)]}{[C_4 + \sin(\omega t + C_3)]^2}, \quad (57)$$

from which it is readily seen that the time-averaged (over a period) of  $N_1$  and  $N_2$  vanishes;  $\langle N_1 \rangle = \langle N_2 \rangle = 0$ .

In Fig. 4 the first normal stress difference  $N_1$  is plotted by using the exact explicit solution. Note that the time-dependent normal stress differences (57) vanish when the vesicle aligns with the flow ( $\psi = 0$ ) and at the orientation  $\psi = \pm\pi/4$ . As a function of  $h$ ,  $\langle N_1 \rangle$  is connected with the angle orientation during the TT regime. It decreases upon decreasing  $h$  (or equivalently increasing  $\lambda$ ) and vanishes at the critical value  $h = h_c$  with a square-root singularity (at the transition a tank-trading vesicle has its main axis parallel to the flow). During the TB and VB regimes  $\langle N_1 \rangle$  remains zero (there is no preferred orientation of the vesicle).

## IV. CONSTITUTIVE LAW IN THE CASE OF AN ARBITRARY LINEAR FLOW

### A. Preliminaries

Our starting point is the evolution equation of the shape conformation and the relation between the stress tensor and the shape conformation. These equations were originally derived in Ref. [15]. We shall rather use the Cartesian form of the conformation of the vesicle instead of  $F_{ij}$  referring to spherical coordinates, used here above. The relation between the two sets

of coefficients is given by

$$\begin{aligned} r &= 1 + \varepsilon \sum_{m=-2}^2 F_{2m}(t) \mathcal{Y}_{nm}(\theta, \phi) \\ &= 1 + \varepsilon \sum_{i,k=x,y,z} 3r_i r_k f_{ik}(t). \end{aligned} \quad (58)$$

Parameter  $\varepsilon$  is a small quantity and can be related to the excess area via  $\varepsilon = \sqrt{\Delta}$ .

The vesicle conformation  $f_{ij}$  equation was derived in Ref. [15] for a shear flow, where the shear plane lies in the  $x$ - $y$  plane. It reads

$$\frac{Df_{ij}}{Dt} = \frac{h}{6} \sqrt{\frac{15}{2\pi}} e_{ij} + 6h \sqrt{\frac{15}{32\pi}} f_{xy} f_{ij}, \quad (59)$$

where  $DM/Dt$  is the Jaumann (or corotational) derivative defined as

$$\frac{DM}{Dt} = \frac{DM}{Dt} + \frac{1}{2} [\omega \mathbf{M} - \mathbf{M} \omega], \quad (60)$$

where  $\mathbf{M}$  is any second-order tensor,  $D/Dt$  is the usual material derivative, and  $\omega = (\nabla \mathbf{v} - \nabla \mathbf{v}^T)/2$  is the vorticity tensor. The nonlinear behavior is present in the  $6h\sqrt{15/(32\pi)}f_{xy}f_{ij}$  term of Eq. (59).

In order to derive a constitutive law we need to generalize this equation to an arbitrary flow. We will assume that the flow gradient remains small enough (i.e., we assume that the flow evolves slowly enough at the scale of the suspended entities), so that at the scale of a vesicle (or RBC) the flow can be regarded as linear shear. However, each vesicle will “see” locally a shear flow which has another orientation than that seen by the other vesicles. This is also the spirit of the derivation of the Oldroyd B constitutive law for dilute polymer solutions [36]. The question thus amounts to extending the derivation to an arbitrary shear flow (having arbitrary orientation).

For an arbitrary orientation of the shear plane, the generalization of the evolution equation (59) takes the form

$$\frac{D\mathbf{f}}{Dt} = \alpha \mathbf{e} + \beta (\mathbf{f} : \mathbf{e}) \mathbf{f}. \quad (61)$$

We have set

$$\alpha = \frac{20}{\sqrt{\Delta}}, \quad \beta = -\frac{192\pi}{(23\lambda + 32)\sqrt{\Delta}}. \quad (62)$$

The relation between the stress tensor  $\sigma$  and the vesicle conformation  $\mathbf{f}$  was derived in Ref. [15] for a shear flow with a given orientation of the axes. The generalization to an arbitrary coordinate system is readily obtained,

$$\frac{\sigma}{2\eta_{\text{ext}}} = \mathbf{e} + \frac{5\phi}{2} \left(1 - \frac{4h}{5} \sqrt{\frac{15}{2\pi}}\right) \mathbf{e} + \phi \sqrt{\frac{15\pi}{2}} \frac{96(\mathbf{f} : \mathbf{e}) \mathbf{f}}{5}, \quad (63)$$

which we will abbreviate as

$$\sigma = \alpha' \mathbf{e} + \beta' (\mathbf{f} : \mathbf{e}) \mathbf{f}, \quad (64)$$

where

$$\begin{aligned} \alpha' &= 2\eta_{\text{ext}} \left[ 1 + \frac{5\phi}{2} \left( 1 - \frac{4h}{5} \sqrt{\frac{15}{2\pi}} \right) \right], \\ \beta' &= \frac{192\eta_{\text{ext}}\phi}{5} \sqrt{\frac{15\pi}{2}}. \end{aligned} \quad (65)$$

The closure condition is given by the momentum balance and mass conservation equations

$$\nabla \cdot \sigma = 0, \quad \nabla \cdot \mathbf{v} = 0. \quad (66)$$

Equations (61)–(64) constitute a closed set for the study of rheology of a dilute suspension of vesicles in the leading-order limit in arbitrary flow provided that the velocity gradient is small on the scale of the suspended entities. The knowledge of  $\mathbf{f}$  from Eq. (61) determines the stress from Eq. (64). Use of the conservation law (66) (plus boundary conditions) determines in principle the flow properties of the complex fluid.

### B. A closed form for the constitutive law

A closed form of the constitutive equation (i.e., relating directly the stress  $\sigma$  to the strain rate  $\mathbf{e}$ ) can be obtained from the equations derived in the previous section. A simple algebraic manipulation of Eqs. (61) and (64) allows us to extract the following relation:

$$(\mathbf{f} : \mathbf{e}) = \pm \sqrt{\frac{\sigma : \mathbf{e} - \alpha' \mathbf{e} : \mathbf{e}}{\beta'}}. \quad (67)$$

Referring to the study performed here, we can check that, in the pure shear flow, the study of tank-treading motion shows that the solution with the minus sign is unstable. Therefore, we select the plus solution. The next step of the derivation consists of applying to Eq. (64) the Jaumann derivative and, by using Eqs. (67) and (61), one obtains a closed form relating the stress and strain rate, which can be written quite as follows:

$$\frac{D\mathbf{S}}{Dt} = (a_1 \mathbf{e} + a_2 \mathbf{S}) \sqrt{\mathbf{S} : \mathbf{e}} + a_3 \frac{\mathbf{S}}{\sqrt{\mathbf{S} : \mathbf{e}}} \frac{D}{Dt} \sqrt{\mathbf{S} : \mathbf{e}}, \quad (68)$$

where  $\mathbf{S} = (\sigma - \alpha' \mathbf{e})$ ,  $a_1 = \alpha \sqrt{\beta'}$ ,  $a_2 = \beta / \sqrt{\beta'}$ , and  $a_3 = \beta'$ .

## V. DISCUSSION OF CONSTITUTIVE LAW AND COMPARISON WITH EMULSION AND CAPSULE SUSPENSIONS

It is worthwhile to briefly compare the present constitutive law (68) with that of emulsions, capsule suspensions, and dilute polymer solutions (Oldroyd B model).

The analog of Ref. (61) for emulsions is given by [37]

$$\varepsilon' \frac{D\mathbf{f}}{Dt} = \frac{5}{3(2\lambda + 3)} \mathbf{e} - \frac{40(\lambda + 1)}{(2\lambda + 3)(19\lambda + 16)} \mathbf{f}, \quad (69)$$

where  $\varepsilon'$  is a small parameter ensuring the small strength of the drop deformation about a sphere. It is shown in Ref. [37] that, generally,  $\varepsilon' \sim \eta_{\text{ext}} \dot{\gamma} r_0 / \Lambda$  (where  $\Lambda$  is the surface tension). This means that the small-deformation theory is valid for a small enough capillary number. The first important difference between Eqs. (69) and (61) is the fact that Eq. (61) is *nonlinear* in the deformation  $\mathbf{f}$ , while it is *linear* for a drop (69). This

is traced back to the local-area constraint for vesicles. It is precisely this nonlinearity that is the source of rich time dynamics and bifurcations for vesicles.

The analog of Eq. (64) in the case of emulsions is given by [37]

$$\frac{\sigma}{2\eta_{\text{ext}}} = \mathbf{e} + \frac{\phi}{2} \left[ \frac{10(\lambda - 1)}{2\lambda + 3} \mathbf{e} + \frac{24}{2\lambda + 3} \mathbf{f} \right]. \quad (70)$$

Here again the equation for vesicles is nonlinear in the deformation, while it is linear for drops. The source of the nonlinearity is again the membrane incompressibility.

Let us now compare our results to the case of inextensible capsule suspensions, which is the closest situation to ours. The evolution equation for the conformation tensor is given by [32]

$$\varepsilon \frac{D\mathbf{f}}{Dt} = \frac{20}{23\lambda + 32} \mathbf{e} - \frac{8}{23\lambda + 32} \mathbf{f}. \quad (71)$$

Here again the same remarks made for emulsion apply: apart from the Jaumann derivative, the equation is linear, in contrast to Eq. (61). This is a bit astonishing. We have seen in the vesicle model that bending energy scales out from the equation at leading order. Likewise, in capsule theory, shear elasticity scales out to leading order for the same reason. Therefore, inextensible capsule and vesicle models should become equivalent to leading order. However, Eq. (5.6) in Ref. [32] [identical to Eq. (71), apart from the constant prefactor] is different from Eq. (61).

We believe that the treatment made for capsules should be revisited as follows: We have to restart from the evolution equation which contains the elastic contribution [Eq. (5.1) in Ref. [32]]. Then, following the same procedure as in Sec. V, one arrives at the same evolution equation for vesicles (59) or for a generalized flow (61). That is to say, at leading order, both systems obey the same equation. To higher order in  $\mathbf{f}$  it is not yet clear how the difference between the two systems expresses itself. Indeed, one expects elasticity to reinstate itself at higher order, as does membrane rigidity in the case of vesicles. Since the physics of the two systems are different, we expect different behaviors. This question is under investigation.

By applying the Jaumann derivative to Eq. (70), and by using Eq. (69) in order to eliminate  $\mathbf{f}$ , it is a simple matter to show that the stress tensor can be related to the strain tensor via a relation of the form

$$\frac{D\sigma}{Dt} + \gamma_1 \sigma = \gamma_2 \mathbf{e} + \gamma_3 \frac{D\mathbf{e}}{Dt}, \quad (72)$$

where constants  $\gamma_1$ ,  $\gamma_2$ , and  $\gamma_3$  are expressed in terms of the coefficients in Eqs. (69) and (70) and are not listed here since we are only interested in comparing the general forms of constitutive laws.

The above relation is reminiscent of the constitutive law for a dilute solution of polymers, treated as a suspension of elastic Hookean dumbbells, commonly known as the Oldroyd B model, which reads [36,38]

$$\sigma_{(1)} + \alpha_1 \sigma = \eta_{\text{ext}} [\mathbf{e} + \alpha_2 \mathbf{e}_{(1)}], \quad (73)$$

where  $\alpha_1$  and  $\alpha_2$  are constants of the model (they are related to friction of the dumbbell with the solvent and the elastic constant of the dumbbell) and the subscript (1) refers to the

upper convected derivative defined as

$$\sigma_{(1)} = \frac{D\sigma}{Dt} - [\nabla v \sigma + \sigma \nabla v^T]. \quad (74)$$

The conformation tensor for a dumbbell is defined as  $\mathbf{f} = \langle \mathbf{RR} \rangle / R_g^2$  where  $\mathbf{R}$  is the end-to-end vector,  $R_g$  is the equilibrium gyration value for a Gaussian polymer chain, and  $\langle \dots \rangle$  designates average over noise due to solvent. The conformation tensor obeys a linear equation of the form

$$\mathbf{f}_{(1)} = \frac{\mathbf{I} - \mathbf{f}}{\tau}, \quad (75)$$

where  $\tau$  is a relaxation time of the polymer towards equilibrium, and  $\mathbf{I}$  is the identity tensor. The Oldroyd B model shares similarities with the emulsions rheology, the major difference being the nature of the time derivative, which have different rheological consequences.

Due to the nonlinear nature of both the equation obeyed by the conformation tensor for vesicles [Eq. (61) at leading order] and the relation between stress and conformation (64), our constitutive law (68) is highly nonlinear and contains rational functions of  $\sigma$  and  $\mathbf{e}$ .

## VI. SUMMARY OF MAIN RESULTS

The major results obtained here are the following:

(i) In addition to the already existing result of the effective viscosity in the TT regime [Eq. (19)], we have been able to derive analytically the instantaneous viscosity for the three classical regimes [Eq. (21)], including the TB and VB ones. We have shown that the time-dependent viscosity has a minimal value [Eq. (30)] which is smaller than the Einstein one.

(ii) We showed that the instantaneous viscosity has a nontrivial behavior as a function of time and exhibits several maxima and minima (as reported numerically before [15,28]) over one period.

(iii) We also analytically obtained the time-averaged (over one period) expression of the effective viscosity. This average expression is given by Eq. (26) and shows a cusp singularity when the viscosity contrast is equal to the critical value  $\lambda_c$  for the transition from TT to TB and VB regimes. This averaged viscosity has a minimum at  $\lambda = \lambda_c$ . As  $\lambda$  is increased, the averaged viscosity decreases in the TT regime and increases in the TB and VB regimes. In the limit of high viscosity contrast we have shown that the reduced viscosity tends to a value equal to 5/2 [see Eq. (31)].

(iv) We compared the reduced effective viscosity of vesicles to that of an initially spherical capsule with a RBC-type membrane. As for vesicles, we have shown that the reduced effective viscosity of capsule has a minimum, even when the capsule is in the TT regime. Moreover, we have shown that the elastic capillary number for capsules and the square root of the excess area play similar roles (at leading order).

(v) We analytically calculated the instantaneous normal stress differences  $N_1$  and  $N_2$  for the three regimes TT, TB, and VB [Eq. (55)]. The behaviors of  $N_1$  and  $N_2$  are nontrivial over one period and capture the previously reported numerical results [15,28].

(vi) We showed that the averaged values of the normal stresses both decrease when  $\lambda$  increases in the TT regime

[Eq. (56)]. When the critical value of  $\lambda$  is approached, we have shown that they exhibit a square-root singularity. We have shown that, in the TB and VB regime, they collapse to zero, in accordance with numerical results [15,28].

(vii) We also determined a constitutive law for a vesicle suspension in a closed form and compared the result with that of emulsions, capsule suspensions, and dilute polymer solutions (Oldroyd B model). The constitutive law is highly nonlinear due to local membrane incompressibility.

## VII. CONCLUSION AND PERSPECTIVES

The purpose of this paper is to reexamine the rheology of a dilute suspension of vesicles. The analysis is analytical and based on the small-deformation theory presented in the original work [13]. In the small-deformation limit, vesicles, under shear flow, exhibit various dynamics, TT, TB and VB modes, depending on viscosity ratio  $\lambda$  and initial conditions. Recently, exact analytical expressions of the vesicle inclination angle and the shape deformation have been discovered [27]. We briefly recalled some features of exact analytical solutions and then derived rheological laws in terms of the effective viscosity and the normal stress differences. Exact analytical expressions of  $\eta_{\text{eff}}$ ,  $N_1$ , and  $N_2$  are presented for the three regimes. In the TB and VB regimes it is clearly found that  $\eta_{\text{eff}}$ ,  $N_1$ , and  $N_2$  are nonlinear oscillating functions of time. In addition, the exact expression of the effective viscosity showed a cusp singularity at the critical viscosity ratio at which TB takes place, whereas the time averages over one

period of the normal stress differences vanish in the TB and VB regimes. In addition, we found that, for large  $\lambda$ , the reduced effective viscosity behaves similar to the drop one. The exact analytical analysis reported here can serve as a starting point for the study of higher-order contributions in the shape deformation equations [16,17], or for the study of incompressible capsules [22,24] (a model for red blood cells). It was numerically shown recently [39] that the study of rheology of vesicles under the combination of a steady shear flow and an oscillating flow exhibits several new features (like resonances in the viscosity as a function of shear rate) that cannot be captured by the application of a pure oscillation. The present analysis can serve as a starting point in order to understand analytically this behavior. It is our hope to investigate this matter further in a future presentation. Finally, we derived a constitutive law in a closed form relating the stress tensor to the strain rate tensor. The form of this law is quite different from other classical laws, such as the popular Oldroyd B model. It will be an interesting task to study systematically this law in various flow configurations and to analyze its far-reaching consequences.

## ACKNOWLEDGMENTS

M. G. and M. B. acknowledge support by the Fond européen de développement régional (FEDER) and the Conseil Régional de Picardie, Project MODCAP. C.M. is grateful to The Centre National d'Etudes Spaciales (CNES) and The European Space Agency (ESA) for financial support.

- 
- [1] P. Vlahovska, T. Podgorski, and C. Misbah, *C. R. Phys.* **10**, 775 (2009).
  - [2] S. R. Keller and R. Skalak, *J. Fluid Mech.* **120**, 27 (1982).
  - [3] M. Kraus, W. Wintz W, U. Seifert, and R. Lipowsky, *Phys. Rev. Lett.* **77**, 3685 (1996).
  - [4] K. H. de Haas, C. Blom, D. van den Ende, M. H. G. Duits and J. Mellema, *Phys. Rev. E* **56**, 7132 (1997).
  - [5] U. Seifert, *Eur. Phys. J. B* **8**, 405 (1999).
  - [6] T. Biben and C. Misbah, *Phys. Rev. E* **67**, 031908 (2003).
  - [7] J. Beaucourt, F. Rioual, T. Séon, T. Biben, and C. Misbah, *Phys. Rev. E* **69**, 011906 (2004).
  - [8] F. Rioual, T. Biben, and C. Misbah, *Phys. Rev. E* **69**, 061914 (2004).
  - [9] H. Noguchi and G. Gompper, *Phys. Rev. Lett.* **93**, 258102 (2004).
  - [10] V. Kantsler and V. Steinberg, *Phys. Rev. Lett.* **95**, 258101 (2005).
  - [11] V. Kantsler and V. Steinberg, *Phys. Rev. Lett.* **96**, 036001 (2006).
  - [12] M. A. Mader, V. Vitkova, M. Abkarian, A. Viallat, and T. Podgorski, *Eur. Phys. J. E: Soft Matter Biol. Phys.* **19**, 389 (2006).
  - [13] C. Misbah, *Phys. Rev. Lett.* **96**, 028104 (2006).
  - [14] P. M. Vlahovska and R. S. Gracia, *Phys. Rev. E* **75**, 016313 (2007).
  - [15] G. Danker and C. Misbah, *Phys. Rev. Lett.* **98**, 088104 (2007).
  - [16] G. Danker, T. Biben, T. Podgorski, C. Verdier, and C. Misbah, *Phys. Rev. E* **76**, 041905 (2007).
  - [17] V. V. Lebedev, K. S. Turitsyn, and S. S. Vergeles, *Phys. Rev. Lett.* **99**, 218101 (2007).
  - [18] H. Noguchi and G. Gompper, *Phys. Rev. Lett.* **98**, 128103 (2007).
  - [19] V. Vitkova, M. A. Mader, B. Polack, C. Misbah, and T. Podgorski, *Biophys. J.* **95**, L33 (2008).
  - [20] G. Danker, C. Verdier, and C. Misbah, *J. Non-Newtonian Fluid Mech.* **152**, 156 (2008).
  - [21] J. Deschamps, V. Kantsler, and V. Steinberg, *Phys. Rev. Lett.* **102**, 118105 (2009).
  - [22] R. Finken, S. Kessler, and U. Seifer, *J. Phys.: Condens. Matter* **23**, 184113 (2011).
  - [23] S. K. Veerapaneni, Y. N. Young, P. M. Vlahovska, and J. Blawdziewicz, *Phys. Rev. Lett.* **106**, 158103 (2011).
  - [24] P. M. Vlahovska, Y. N. Young, G. Danker, and C. Misbah, *J. Fluid Mech.* **678**, 221 (2011).
  - [25] W. Helfrich, *Z. Naturforsch* **28c**, 693 (1973).
  - [26] M. Thiébaud and C. Misbah, *Phys. Rev. E* **88**, 062707 (2013).
  - [27] M. Guedda, M. Abaidi, M. Benlahsen, and C. Misbah, *Phys. Rev. E* **86**, 051915 (2012).
  - [28] G. Gighliotti, T. Biben, and C. Misbah, *J. Fluid Mech.* **653**, 489 (2010).
  - [29] A. Einstein, *Ann. Phys. (Leipzig)* **19**, 289 (1906); **34**, 591 (1911).
  - [30] J. F. Brady, *Int. J. Multiphase Flow* **10**, 113 (1983).
  - [31] P. Bagchi and R. M. Kalluri, *Phys. Rev. E* **81**, 056320 (2010).

- [32] D. Barthes-Biesel and J. M. Rallison, *J. Fluid. Mech.* **113**, 251 (2006); A. Drochon, *Eur. Phys. J.: Appl. Phys.* **22**, 155 (2003).
- [33] D. Barthes-Biesel, *Biomat. Artif. Cells, Blood Substitutes, Immobilization Biotechnol.* **21**, 359 (1993).
- [34] A. P. Spann, H. Zhao, and E. S. Shaqfeh, *Phys. Fluids* **26**, 031902 (2014).
- [35] D. Barthes-Biesel and V. Chhim, *Int. J. Multiphase Flow* **7**, 493 (1981).
- [36] R. B. Bird, R. C. Armstrong, and O. Hassager, *Dynamics of Polymeric Liquids, Vol. 1, Fluid Dynamics* (Wiley, New York, 1977).
- [37] N. A. Frankel and A. Acrivos, *J. Fluid Mech.* **44**, 65 (2006).
- [38] R. Larson, *The Structure and Rheology of Complex Fluids* (Oxford University Press, Oxford, 1999).
- [39] A. Farutin and C. Misbah, *J. Fluid Mech.* **700**, 362 (2012).